Received: 28 April 2021 | Revised: 10 August 2021 | Accepted: 31 August 2021

DOI: 10.1002/ijc.33809

TUMOR IMMUNOLOGY AND MICROENVIRONMENT

IJC International Journal of Cancer

A quantitative polymerase chain reaction based method for molecular subtype classification of urinary bladder cancer—Stromal gene expressions show higher prognostic values than intrinsic tumor genes

Csilla Olah[1] | Christina Hahnen[1] | Nikolett Nagy[2] | Joanna Musial[1] | Melinda Varadi[2] | Gabor Nyiro[3] | Balazs Gyorffy[4,5] | Boris Hadaschik[1] | Josefine Rawitzer[6] | Saskia Ting[6] | Gottfrid Sjödahl[7] | Michéle J. Hoffmann[8] | Henning Reis[7] | Tibor Szarvas[1,2]

[1]Department of Urology, University of Duisburg-Essen, Essen, Germany

[2]Department of Urology, Semmelweis University, Budapest, Hungary

[3]MTA-SE Molecular Medicine Research Group, Semmelweis University, Budapest, Hungary

[4]2nd Department of Pediatrics and Department of Bioinformatics, Semmelweis University, Budapest, Hungary

[5]Research Centre for Natural Sciences, Cancer Biomarker Research Group, Institute of Enzymology, Budapest, Hungary

[6]Institute of Pathology, University Medicine Essen, University of Duisburg-Essen, Essen, Germany

[7]Department of Oncology, Clinical Sciences, Lund University Hospital, Lund University, Lund, Sweden

[8]Department of Urology, Medical Faculty, Heinrich-Heine-University Duesseldorf, Duesseldorf, Germany

Correspondence
Tibor Szarvas, Department of Urology, University of Duisburg-Essen, University Hospital Essen, 45147 Essen, Germany.
Email: tibor.szarvas@uk-essen.de

Funding information
Wilhelm Sander-Stiftung, Grant/Award Number: D/106-22012; Ministry for Innovation and Technology in Hungary, Grant/Award Numbers: 2020-4.1.1.-TKP2020, 2018-1.3.1-VKE-2018-00032, 2018-2.1.17-TET-KR-00001; Ministry for Innovation and Technology from the source of the National Research Development and Innovation Fund, Grant/Award Number: K139059; New National Excellence Program, Grant/Award Numbers: ÚNKP-20-5-SE-1, ÚNKP-21-5-SE-3; János Bolyai Research Scholarship of the Hungarian Academy of Sciences

Abstract

Transcriptome-based molecular subtypes of muscle-invasive bladder cancer (MIBC) have been shown to be both prognostic and predictive, but are not used in routine clinical practice. We aimed to develop a feasible, reverse transcription quantitative polymerase chain reaction (RT-qPCR)-based method for molecular subtyping. First, we defined a 68-gene set covering tumor intrinsic (luminal, basal, squamous, neuronal, epithelial-to-mesenchymal, in situ carcinoma) and stromal (immune, extracellular matrix, p53-like) signatures. Then, classifier methods with this 68-gene panel were developed in silico and validated on public data sets with available subtype class information (MD Anderson [MDA], The Cancer Genome Atlas [TCGA], Lund, Consensus). Finally, expression of the selected 68 genes was determined in 104 frozen tissue samples of our MIBC cohort by RT-qPCR using the TaqMan Array Card platform and samples were classified by our newly developed classifiers. The prognostic value of each subtype classification system and molecular signature scores were assessed. We found

Abbreviations: BC, bladder cancer; CIS, *carcinoma* in situ; CSS, cancer-specific survival; ECM, extracellular matrix; EMT, epithelial-to-mesenchymal transition; IHC, immunohistochemical; MDA, MD Anderson; MIBC, muscle-invasive bladder cancer; NAC, neoadjuvant chemotherapy; OS, overall survival; RC, radical cystectomy; TCGA, The Cancer Genome Atlas.

that the reduced marker set combined with the developed classifiers were able to reproduce the TCGA II, MDA, Lund and Consensus subtype classification systems with an overlap of 79%, 76%, 69% and 64%, respectively. Importantly, we could successfully classify 96% (100/104) of our MIBC samples by using RT-qPCR. Neuronal and luminal subtypes and low stromal gene expressions were associated with poor survival. In conclusion, we developed a robust and feasible method for the molecular subtyping according to the TCGA II, MDA, Lund and Consensus classifications. Our results suggest that stromal signatures have a superior prognostic value compared to tumor intrinsic signatures and therefore underline the importance of tumor-stroma interaction during the progression of MIBC.

KEYWORDS

bladder cancer, molecular subtype classification, neuronal signature, stroma

What's new?

Transcriptome-based molecular subtypes of muscle-invasive bladder cancer have been demonstrated to be both prognostic and predictive. However, due to their complexity and high costs, transcriptome-based methods are not used in routine clinical practice. Here, the authors present a feasible 68-gene panel- and RT-qPCR-based method for molecular subtyping according to the most commonly used molecular classification systems of muscle-invasive bladder cancer. The method has been validated using *in silico* datasets and was further tested in an institutional bladder cancer cohort. The data revealed different prognoses for some of the molecular subgroups and underlined the prognostic relevance of stroma-related gene expression signatures.

1 | INTRODUCTION

Bladder cancer (BC) is a common malignancy with approximately 550 000 new cases each year worldwide.[1] Urothelial carcinoma is the most frequently diagnosed histological type of BC. About 30% of cases are muscle-invasive at first presentation or will ultimately progress to muscle-invasive bladder cancer (MIBC). The standard care of MIBC is radiochemotherapy or radical cystectomy (RC) with perioperative platinum-based chemotherapy; however, the 5-year survival rate of these patients is less than 50%. Currently, checkpoint and fibroblast growth factor receptor (FGFR) inhibitors as well as Nectin-4 antibody conjugates have become available for platinum-resistant and/or -ineligible patients. Only few routinely available predictive biomarkers, such as Programmed death-ligand 1 expression by immunohistochemistry or *FGFR3* mutational or fusion-status, are available.[2-4] MIBC patients may show remarkable differences regarding their response to therapies. Therefore, a more detailed characterization of MIBC is required to decipher this clinical heterogeneity.

In the last years, several studies demonstrated that MIBCs with similar histological patterns may have distinct molecular properties. Transcriptome analyses of MIBC samples revealed distinct molecular subtypes with different prognosis. One of the earliest molecular classifications was developed by a research group from Lund and distinguished five subtypes with diverse gene expression patterns and clinical outcome.[5] Then the "University of North Carolina (UNC) classification" defined luminal and basal subtypes similarly to the determined subtypes in breast cancer and revealed that luminal tumors have a significantly better prognosis compared to basal cases.[6] Subsequent studies confirmed the presence of luminal and basal subtypes in independent MIBC cohorts. The "MD Anderson (MDA) classification" described a p53-like subtype in addition to luminal and basal subtypes, which was associated with an improved survival compared to basal tumors; however, it showed resistance to chemotherapy.[7] In addition, Seiler et al found that only patients classified as basal subtype benefited from a platinum-based neoadjuvant chemotherapy (NAC).[8] In the first The Cancer Genome Atlas (TCGA) study in 2014, 129 MIBC samples were analyzed by transcriptome sequencing,[9] which in 2017 has been extended to 412 samples. This "TCGA II" study distinguished three luminal (luminal-infiltrated, luminal-papillary and luminal), a basal/squamous and a neuronal subtype.[10] Of these molecular subgroups, neuronal tumors had the worst while the luminal-papillary tumors exhibited the most favorable prognosis. Recently, an international consensus classification with six molecular subtypes has been suggested based on a reanalysis of 1750 formerly published MIBC transcriptome profiles.[11] This study included an own nomenclature with significant overlap with previously suggested classification systems. The authors confirmed a more favorable prognosis for luminal papillary subtype, as well as for the luminal nonspecified and stroma-rich subtypes, while luminal unstable, basal/squamous and neuronal subtypes had a poor prognosis. However, no significant differences could be observed in NAC-treated patients regarding the outcomes between various consensus subtypes.

All these subtype classification systems are based on transcriptome data and consider the expression of thousands of genes, which is hardly compatible with daily clinical routine. Therefore, we aimed to develop a simple and applicable system for potential inclusion in daily clinical routine with the final aim to translate the molecular findings to clinical application. To achieve this, we utilized a reverse transcription quantitative polymerase chain reaction (RT-qPCR)-based gene expression analysis method with a reduced marker set and a respective evaluation method in order to recapitulate the TCGA II, MDA, Lund and Consensus subtype classifications. The marker set and the classifier method was developed in silico and then validated in respective published data sets. Then gene expression levels of the selected markers were determined by RT-qPCR in frozen tissue samples of 104 MIBC patients and the prognostic value of the subtype classification as well as various stromal and tumor intrinsic gene signatures were correlated with clinical and follow-up data.

2 | MATERIALS AND METHODS

2.1 | Development of a classifier method for molecular subtyping using a reduced marker set

First, we selected the markers as the genes with the highest discriminating effect between distinct molecular subtypes in the TCGA II study. Then, identified marker set were further reduced and those markers also used in other classification systems were preferred. Based on a comparison of respective subtype classification studies, a panel of 68 genes was defined in order to distinguish molecular subtypes according to the TCGA II, MDA, Lund and Consensus systems.[7,10-13] These markers covered six tumor cell-specific and three stroma-related gene signatures (Table 1). The tumor intrinsic signatures were as follows: luminal, basal, squamous, neuronal, epithelial-to-mesenchymal transition (EMT), *carcinoma* in situ (CIS), while stroma-specific signatures included p53, extracellular matrix (ECM)/smooth muscle and immune cell-specific genes.[10]

Second, we used respective publicly available data sets for the in silico development and validation of subtype classification rule sets for the TCGA II, MDA, Lund and Consensus classification systems. For each classification system, two data sets with available transcriptome-based subtype class information were used for the elaboration (training set) and validation (validation set) of our classifier method (Figures 1, S1A, S3A and S5A).

From the publicly available data sets, gene expression data for the 68 genes were filtered for further analysis. For each of the 68 genes, an expression score (ranging from 1 to 5) was calculated based on their relative expression in the given patient cohort. For this, an automatic cutoff generation was applied for each gene resulting in equal percentiles (20%) of patients in each group. For each sample, signature scores (basal/squamous, luminal, neuronal, CIS, ECM, EMT, p53-like, immune) were calculated as the mean value of the respective gene expression scores (Table 1). A stepwise classification of samples was optimized on the training sets by adjusting two parameters, cutoffs for signature scores and the sequence of selection steps into different subtype groups. These two parameters were adjusted until the highest overlap with the original transcriptome-based classification was reached. The so developed classifier rule sets were applied to the training sets to validate their overlap in a second cohort (Figures 1, S1A, S3A and S5A).

For the definition of the TCGA II classifier rule set, we randomly divided the TCGA data set (https://tcga-data.nci.nih.gov/tcga/) into a training set (n = 203) and a validation set (n = 202),[10] for the MDA classification we used the GSE48075 data set (discovery cohort) as the training cohort (n = 73) and the TCGA data set as the validation cohort (n = 231),[7,14] for the Lund classification, the GSE83586 data set was divided into a training (n = 154) and a validation cohort (n = 153).[12] For the Consensus classification, we divided again the TCGA data set into a training (n = 201) and a validation set (n = 202). In addition, the gene panel-based Consensus classifier was further validated on the MDA (n = 73),[7] Lund (n = 307),[12] CIT (n = 85, E-MTAB-1803),[15] Riester (n = 78, GSE31684)[16] and Seiler (n = 305, GSE87304)[8] cohorts,

TABLE 1 Selected 68-gene marker set assigned to signatures and to classification systems as they were applied [Color table can be viewed at wileyonlinelibrary.com]

TCGA II	MDA	Lund	Consensus	Signature	Selected genes									
X	X	X	X	Luminal	CYP2J2	ERBB2	ERBB3	FGFR3	FOXA1	GATA3	KRT20	PPARG	UPK1A	UPK2
X	X	X	X	Basal	CD44	CDH3	COL17A1	KRT1	KRT14	KRT16	KRT5	KRT6A	KRT6B	
X	X	X	X	Squamous	DSC2	DSC3	DSG2	DSG3	GSDMC	PI3	TGM1	TP63		
X	–	X	X	Neuronal-diff.	CHGA	CHGB	ENO2	GNG4	NCAM1	PEG10	PLEKHG4B	SCG2	SOX2	TUBB2B
X	–	–	X	CIS	CRTAC1	CTSE	MSN	NR3C1	PADI3					
X	X	–	X	EMT	CDH2	SNAIL	TWIST1	VIM	ZEB1	ZEB2				
X	X	–	X	ECM/SM	C7	COMP	SFRP4	SGCD						
X	–	–	–	Immune	CD274	CXCL11	IDO1	L1CAM	PDCD1LG2	SAA1				
–	X	–	–	p53	MYH11	DES	PGM5	ACTC1	ACTG2	CNN1	FLNC	MFAP4	PCP4	
–	–	X	X	Additional	CDKN2A									
X	X	X	X	Housekeeping	TBP	GAPDH								

Note: "X" marks—signature-scores used for each subtype classification systems (eg, p53-associated genes were only used for the MDA but not for the TCGA, Lund and Consensus classifications, while *CDKN2A* was used for the Lund and Consensus classifications and was additionally measured only in cases [n = 64] when enough RNA samples remained after the first analysis).
Abbreviations: CIS, *carcinoma* in situ; ECM, extracellular matrix; EMT, epithelial-to-mesenchymal transition; MDA, MD Anderson; SM, smooth muscle; TCGA, The Cancer Genome Atlas.

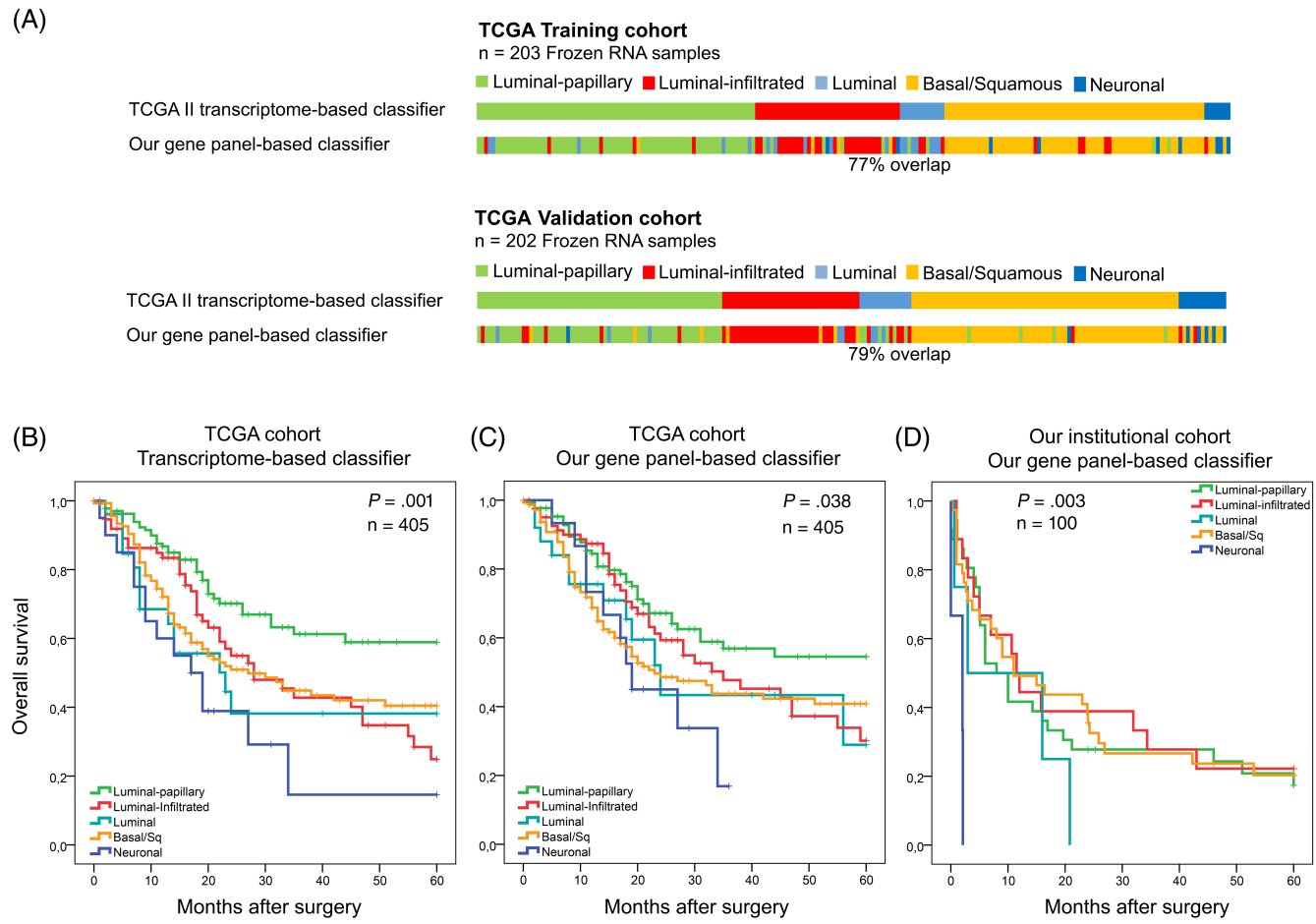

FIGURE 1 Overlap between transcriptome-based, original TCGA molecular subtypes and by our 68 gene-based TCGA II classifier rule set in the training and validation cohorts (A). Kaplan-Meier curve of the original, transcriptome-based TCGA II classification (B). Kaplan-Meier curves using our classifier method on the TCGA cohort (C) and on our institutional cohort (D). TCGA, The Cancer Genome Atlas [Color figure can be viewed at wileyonlinelibrary.com]

which data sets were used for the development and validation of the original Consensus classifier (Figures 1, S1A, S3A and S5A).

2.2 | Institutional patient cohort

Frozen tumor tissue samples from MIBC patients who underwent RC between 1990 and 2005 at the Department of Urology at University of Duisburg-Essen were cut and stained with hematoxylin and eosin for histological evaluation by a GU-pathologist (H. R). Inclusion criteria were: detrusor muscle-invasive (≥T2) urothelial BC, no chemotherapy before cystectomy, ≥50% tumor cell content in the tumor tissue, available follow-up data. Overall, 104 MIBC samples met these criteria. The main characteristics of patients' cohort are given in Table 2.

CDKN2A gene expression was used for the Lund and Consensus classifications and was additionally measured only in cases (n = 64) when enough RNA samples remained after the first analysis. The study was performed according to the Declaration of Helsinki and the institutional ethics committee approved the study protocol (08-3942-BO/15-6400-BO.)

2.3 | RNA extraction, reverse transcription and gene expression analysis by RT-qPCR

RNA isolation was carried out by the RNeasy Kit (Qiagen, Hilden, Germany) according to the manufacturer's protocol with minor modification as described earlier.[17] From each sample, 500 ng RNA was reverse transcribed using the Multiscribe Reverse Transcriptase Kit (Thermo Fisher Scientific, Waltham, MA). Gene expression levels of selected 68 genes and two housekeeping genes (*GAPDH* and *TBP*) were measured by TaqMan Gene Expression Assay using the 364-well TaqMan Array Card platform on QuantStudio 7 Flex Real-Time PCR System (Applied Biosystems, Life Technologies, Thermo Fisher Scientific) according to manufacturer's protocol. Relative gene expression levels were calculated in relation to the expression of the housekeeping gene according to the ΔCt method (Ct [gene of interest] − (Ct [housekeeping gene]) per sample and gene. Based on the ΔCt values, a reverse scale was calculated and samples were divided into five groups by an automatic cutoff generation resulting in equal percentiles (20%) of samples for each assessed gene (1—the lowest, 5—the highest gene expression). Signature scores were calculated as described above (Table 1).

TABLE 2 Patients' characteristics

Variables		Present study (Essen) n (%)	TCGA n (%)	MDA n (%)	Lund n (%)	CIT n (%)	Riester n (%)	Seiler n (%)
Age, median [range]		65 [36-95]	69 [34-90]	69 [n.a.]	70 [38-87]	69 [44-89]	69 [41-92]	69 [22-84]
Sex (male)		69 (69)	304 (74)	54 (74)	240 (78)	70 (82)	n.a.	215 (70)
Examined BCa samples		100	408	73	307	85	78	305
Initial tissue		Frozen	Frozen	Frozen	FFPE	Frozen	Frozen	FFPE
Stage	≤pT1	0	1 (∼0.2)	10 (14)	40 (13)	0	14 (18)	0
	pT2	23 (23)	123 (30)	10 (14)	126 (41)	31 (36)	51 (65)	143 (47)
	pT3	45 (45)	196 (48)	25 (34)	86 (28)	35 (41)	10 (13)	109 (36)
	pT4	32 (32)	59 (14)	12 (16)	28 (9)	19 (22)	3 (4)	49 (16)
	pTx	0	33 (8)	16 (22)	6 (2)	0	0	0
	n.a.	–	–	–	21 (7)	–	–	4 (1)
Metastases	N+	35 (35)	132 (32)	23 (32)	14 (∼5)	28 (33)	n.a.	91 (30)
	M+	4 (4)	11 (∼3)	n.a.	0 (0)	32 (38)	n.a.	n.a.
Chemotherapy	NAC	0	12	18 (25)	0	0	3 (4)	305 (100)
	AC	15 (15)	n.a.	n.a.	n.a.	n.a.	16 (20)	0
OS (patients alive)	1 y	45 (45)	328 (81)	54 (78)	n.a.	67 (79)	69 (89)	n.a.
	2 y	31 (31)	263 (65)	45 (62)	n.a.	55 (65)	67 (86)	n.a.
	3 y	27 (27)	246 (60)	43 (59)	n.a.	52 (61)	65 (83)	n.a.
	4 y	24 (24)	240 (59)	39 (53)	n.a.	50 (59)	65 (83)	n.a.
	5 y	22 (22)	236 (58)	39 (53)	n.a.	48 (56)	64 (82)	n.a.
mRNA profiling method		TaqMan Array Card	Illumina HiSeq	Illumina HiSeq	Affy HG 1.0 ST	Affy U133p2	Affy U133p2	Affy HG 1.0 ST
TGGA II	LumP	36 (36)	141 (35)	–	–	–	–	–
	LumI	18 (18)	76 (19)	–	–	–	–	–
	Lum	4 (4)	26 (6)	–	–	–	–	–
	Ba/Sq	39 (39)	142 (35)	–	–	–	–	–
	Ne	3 (3)	20 (5)	–	–	–	–	–
MDA	Luminal	36 (36)	–	24 (33)	–	–	–	–
	Basal	27 (27)	–	23 (32)	–	–	–	–
	p53-like	37 (37)	–	26 (36)	–	–	–	–
Lund	Uro-like	27 (42)	–	–	133 (43)	–	–	–
	Gen. unstable	7 (11)	–	–	66 (21)	–	–	–
	Infiltrated	–	–	–	6 (2)	–	–	–
	Basal/SCC-like	20 (31)	–	–	62 (20)	–	–	–
	Mes-like	5 (8)	–	–	16 (5)	–	–	–
	SC/Ne-like	5 (8)	–	–	24 (8)	–	–	–
Consensus	LumP	17 (17)	127 (32)	18 (25)	63 (20)	15 (18)	16 (23)	69 (23)
	LumNS	6 (6)	20 (5)	7 (10)	39 (13)	6 (7)	2 (∼3)	24 (8)
	LumU	10 (10)	53 (13)	10 (14)	48 (16)	8 (9)	8 (10)	76 (25)
	Stroma-rich	1 (1)	45 (11)	8 (11)	57 (19)	18 (21)	14 (18)	18 (6)
	Ba/Sq	29 (29)	152 (38)	30 (41)	88 (29)	34 (40)	34 (44)	114 (37)
	Ne-like	1 (1)	6 (∼1.5)	0 (0)	12 (4)	4 (5)	4 (5)	4 (∼1)

Abbreviations: AC, adjuvant chemotherapy; Affy, Affymetrix; Ba/Sq, basal/squamous; BC, bladder cancer; FFPE, formalin-fixed paraffin-embedded; Gen. unstable, genomically unstable; Lum, luminal; LumI, luminal-infiltrated; LumNS, luminal nonspecified; LumP, luminal-papillary; LumU, luminal unstable; M+, distant metastasis; MDA, MD Anderson; Mes, mesenchymal; n.a., not available data; N+, lymph node metastasis; NAC, neoadjuvant chemotherapy; Ne, neuronal; Ne-like, neuroendocrine-like; OS, overall survival; Sc/Ne-like, small-cell/neuroendocrine-like; SCC, squamous cell carcinoma; TCGA, The Cancer Genome Atlas; Uro, urothelial.

2.4 | Statistical analysis

The correlation between TCGA II "summa luminal" (luminal-papillary, luminal-infiltrated, luminal) and basal molecular subtypes and clinicopathological parameters was examined using Pearson's chi-square test. Overall survival (OS) and cancer-specific survival (CSS) were analyzed by univariable Cox analysis and visualized by drawing a Kaplan-Meier plot. For multivariable analysis, Cox regression models were used including parameters reaching *P* value of <.05 in the univariable analysis. Gene expression patterns were visualized on heatmaps (Morpheus, https://software.broadinstitute.org/morpheus). All statistical analyses were performed using the SPSS software package (IBM SPSS Statistics for Windows, version 25, IBM Corp., Armonk, NY).

3 | RESULTS

3.1 | In silico development and validation of a subtype classification method with a reduced marker set

Our classifier rule set was established on the training set, and subsequently validated on the validation set (Figure 1A). We found high overlap between our classification method and the original transcriptome-based TCGA II classification in both the training (77%) and the validation set (79%).

Using the same approach, we developed and validated classifier rule sets for the MDA, Lund and Consensus classification systems. Our method reached 81% and 76% overlap for the MDA classification in the training and the validation set, respectively[14] (Figure S1A). The overlap between our classifier method for the Lund classification proved to be 65% and 69% in the training and validation cohorts, respectively (Figure S3A).[12] Finally, the overlap between the developed Consensus classifier method reached 75% overlap in the training and 70% in the TCGA validation cohorts, respectively (Figure S5A). In addition, an extended validation with the total samples of the TCGA, MDA, Lund, CIT, Riester and Seiler cohorts (number of total samples = 1251) reached 64% comparison between the transcriptome- and gene panel-based classifiers. Supporting Information included the detailed overlaps and distributions of Consensus subtypes (Table S1).

3.2 | Patients' characteristics

The main characteristics of our institutional (Essen cohort) and the other data set cohorts (TCGA II, MDA, Lund, CIT, Riester, Seiler) are summarized in Table 2. In our cohort, the median follow-up time was 10 months with a maximum of 186 months. The Essen and TCGA II cohorts were comparable regarding the median age (65 vs 69), the male ratio (69% vs 74%), the presence of lymph node (35% vs 32%) and distant metastases (4% vs 3%). On the other hand, our institutional cohort contained a higher rate of pT4 tumors compared to the TCGA II cohort (32% vs 14%), which at least partly may explain the shorter survival rate in our cohort. Furthermore, in our institutional cohort, none of the patients received NAC, while 15 patients received postoperative, adjuvant chemotherapy. The MDA, Lund and Riester cohorts included also non-muscle-invasive BCs, while the Seiler cohort included NAC samples, which makes a direct comparison between these and our cohorts difficult.

3.3 | Molecular subtype classification of our institutional cohort and its correlations with clinicopathological parameters

Gene expression of the reduced marker set was determined by RT-qPCR and applied for molecular subtype classification according to our above-described TCGA II classifier rule set. During RT-qPCR data evaluation, four samples were excluded because their low housekeeping gene expression level (Ct >33), leaving 100 samples for the final evaluation (Figure 2). The subtype distribution within our institutional cohort proved to be remarkably similar to that of the TCGA cohort (Table 2). Signature scores were characteristic for respective subgroups (eg, luminal score for luminal groups and basal/squamous score basal/squamous group and neuronal score for neuronal subgroup; Figures S2, S4 and S6). In addition, high level of immune infiltration was characteristic for luminal-infiltrated and basal/squamous subtypes (Figures 2 and S7).

Pearson's chi-square test was used to examine the association between "summa luminal" (luminal-papillary, luminal-infiltrated, luminal), basal/squamous subtypes and main clinicopathological parameters (Table S2). Similar to the findings made in the TCGA cohort, basal subtype tended to associate with female sex and was more frequent in high-stage tumors; however, these correlations proved not to be statistically significant.

3.4 | Survival analysis of clinicopathological parameters and signature scores

Univariable analysis of our institutional cohort revealed lymph node metastasis as a significant risk factor for survival (OS and CSS: $P < .001$). Patients' age and sex had no significant impact on OS and CSS, while tumor stage significantly correlated with CSS ($P = .014$) (Table 3A). Basal, squamous, luminal, CIS and EMT signatures had no significant effect on OS and CSS (Table 3A), while high neuronal scores correlated with poor survival (OS and CSS: $P < .001$). In addition, high ECM, immune and p53-related gene expression scores associated with improved OS ($P = .001$, $P = .001$ and $P = .023$) and CSS ($P = .002$, $P = .006$ and $P = .004$). Multivariable analysis revealed the presence of lymph node metastases, high neuronal and low immune signature scores as independent predictors of poor OS ($P < .001$, $P < .001$ and $P = .039$) (Table 3B). Furthermore, lymph node metastasis, high neuronal and low ECM scores were independent risk factor for CSS ($P < .001$, $P < .001$ and $P = .049$). As a continuous variable, EMT, ECM, immune and p53

signatures correlated with OS ($P = .033$, $P = .004$, $P = .008$ and $P = .011$), moreover ECM, immune and p53 signatures with CSS ($P = .004$, $P = .006$ and $P = .010$) (Table S3A). In addition, multivariable analyses showed that immune signature revealed independent risk factor for OS ($P = .045$) and tended to associate with improved CSS ($P = .070$) (Table S3B).

In order to exclude the possible influencing effect of chemotherapy use on results, we performed survival analyses also after the exclusion of 15 patients who received postoperative platinum therapy. In this cohort, univariable analysis of clinicopathological parameters, signature scores and survivals revealed the same associations as for the whole cohort; lymph node metastasis, neuronal, ECM, immune and p53 score correlated with OS ($P = .002$, $P < .001$, $P = .001$, $P = .001$ and $P = .015$, respectively) and CSS ($P < .001$, $P < .001$, $P = .004$, $P = .002$ and $P = .025$) (Table S4A). Furthermore, multivariable analysis showed that the presence of lymph node metastases and high neuronal scores were independently associated with poor OS and CSS ($P = .001$, $P < .001$ and

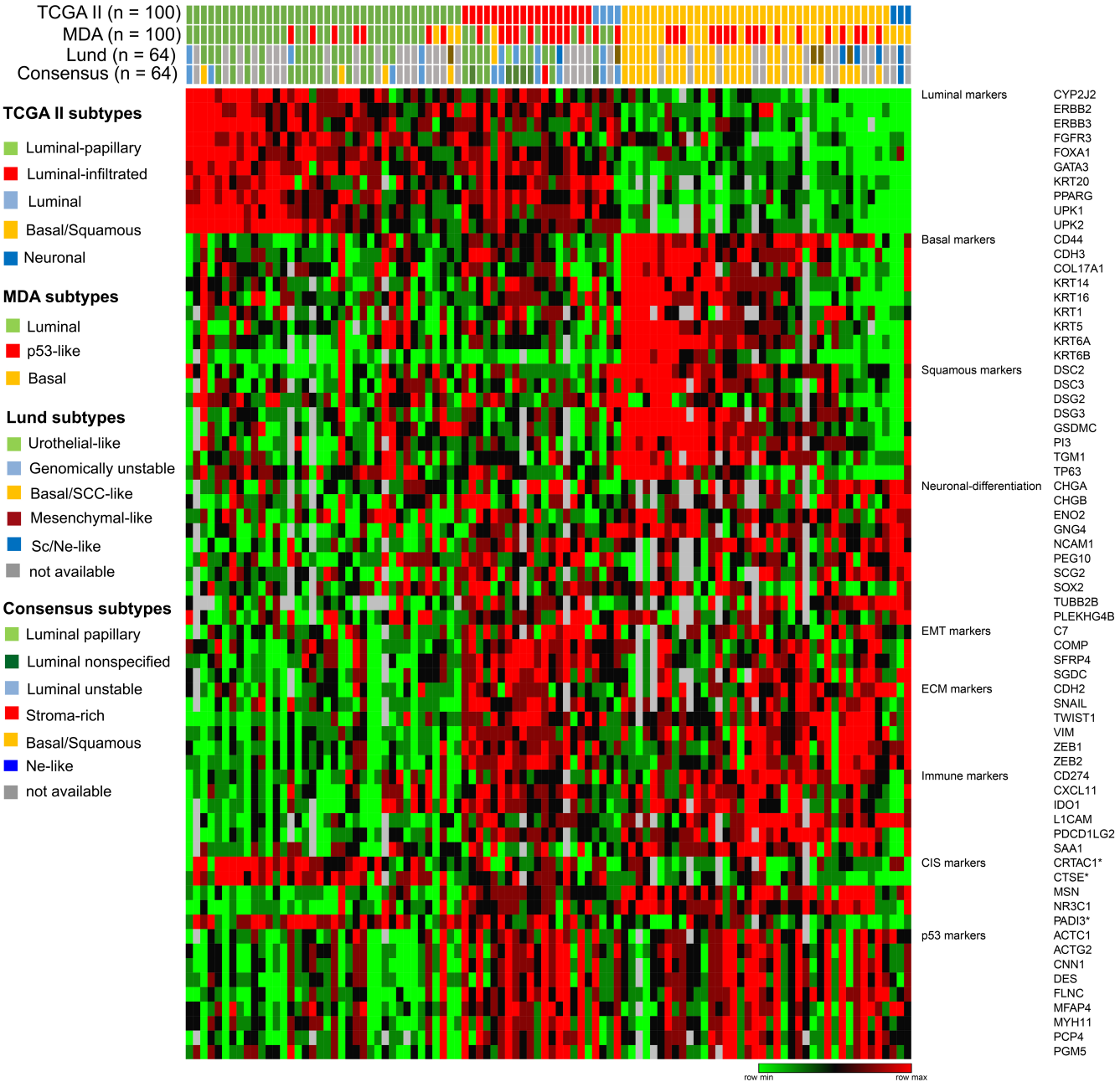

FIGURE 2 Molecular subtypes and their distinct gene expression profile in our institutional cohort visualized by heatmap. The subtypes were determined by our newly developed 68-gene classifier method for the TCGA II, MDA, Lund and Consensus classification systems. *Genes that are downregulated in CIS. CIS, *carcinoma* in situ; MDA, MD Anderson; Ne-like, neuroendocrine-like; Sc/Ne-like, small-cell/neuroendocrine-like; TCGA, The Cancer Genome Atlas [Color figure can be viewed at wileyonlinelibrary.com]

$P < .001$, $P < .001$, respectively) (Table S4B). In addition, low ECM score was correlated with worse OS ($P = .039$), while low immune score tended to associate also with poor OS and significantly correlated with shorter CSS ($P = .071$ and $P = .040$).

3.5 | Survival analysis by the molecular subtype classifications

The original, transcriptome-based subtype classification of the TCGA II cohort proved to be prognostic ($P = .001$); patients with luminal-papillary subtypes showed the most favorable prognosis, while neuronal and luminal subtypes had the worst OS (Figure 1B). Similarly, when classifying the TCGA cohort by our selected marker and rule set, distinct subtypes had significantly different survival rates ($P = .038$) (Figure 1C). Subtype classification of our institutional cohort using the RT-qPCR-based gene expression data also proved to be prognostic ($P = .003$). Similar to the findings of the TCGA study, we found the worst prognosis for the neuronal and luminal subtypes. The other three subtypes did not show a significant difference regarding their OS rates. (Figure 1D). According to the univariable analysis, only neuronal subtypes associated with survival, and was a significant risk factor for OS and CSS ($P = .002$ and $P = .001$) (Table S5).

Survival analysis using our MDA classifier rule set resulted in a similar significant risk stratification compared to the transcriptome-based classification on the reference TCGA cohort ($P = .002$) (Figure S1B,C). The same method on our institutional cohort using our RT-qPCR generated gene expression data revealed the p53-like subtype to have a more favorable prognosis, which is in line with the findings of the MDA study (Figure S1D).[7] The classifier according to Lund subtyping had no significant impact on OS ($P = .203$) (Figure S3B).

TABLE 3 Cox univariable (A) and multivariable (B) survival analyses with dichotomized signature scores of our institutional cohort

A. Univariable analysis						
	Overall survival (n = 100)			**Cancer-specific survival (n = 100)**		
Variables	**HR**	**95% CI**	***P* value**	**HR**	**95% CI**	***P* value**
Age (>65)	1.064	0.671-1.687	.792	0.978	0.597-1.602	.929
Sex (female)	1.548	0.915-2.620	.103	1.498	0.848-2.647	.164
Stage (>pT3)	1.137	0.974-1.328	.104	1.835	1.131-2.977	**.014**
Metastases						
Lymph node (N+)	2.429	1.516-3.892	**<.001**	3.004	1.823-4.950	**<.001**
Distant (M+)	1.645	0.567-4.766	.359	1.881	0.641-5.520	.250
Signature scores						
Basal score (≥3)	0.893	0.571-1.399	.622	0.761	0.472-1.227	.262
Squamous score (≥3)	1.059	0.679-1.652	.800	0.980	0.610-1.573	.993
Basal/squamous score (≥3)	1.002	0.771-1.302	.989	0.881	0.548-1.416	.602
Luminal score (≥3)	1.014	0.652-1.578	.949	1.053	0.655-1.694	.830
Neuronal score (≥4.2)	9.714	3.221-29.291	**<.001**	14.160	4.758-41.822	**<.001**
EMT score (≥3)	0.705	0.452-1.099	.123	0.705	0.438-1.134	.149
ECM score (≥3)	0.450	0.283-0.714	**.001**	0.468	0.289-0.759	**.002**
Immune score (≥3)	0.468	0.296-0.738	**.001**	0.510	0.315-0.826	**.006**
CIS score (≥3)	0.841	0.540-1.310	.444	0.811	0.503-1.309	.392
p53 score (≥3)	0.592	0.376-0.931	**.023**	0.489	0.300-0.798	**.004**
B. Multivariable analysis						
Variables	**HR**	**95% CI**	***P* value**	**HR**	**95% CI**	***P* value**
Stage (>pT3)	—	—	—	1.193	0.718-1.983	.496
Lymph node (N+)	2.484	1.528-4.039	**<.001**	3.178	1.863-5.241	**<.001**
Neuronal score (≥4.2)	12.091	3.602-40.582	**<.001**	16.376	4.852-55.276	**<.001**
ECM score (≥3)	0.607	0.362-1.019	.059	0.551	0.305-0.997	**.049**
Immune score (≥3)	0.569	0.334-0.971	**.039**	0.687	0.391-1.206	.191
p53 score (≥3)	0.886	0.506-1.552	.673	0.739	0.399-1.369	.336

Note: *P* values with bold type are statistically significant (<.05).

Abbreviations: CI, confidence interval; CIS, *carcinoma* in situ; ECM, extracellular matrix; EMT, epithelial-to-mesenchymal transition; HR, hazard ratio; Ref., referent.

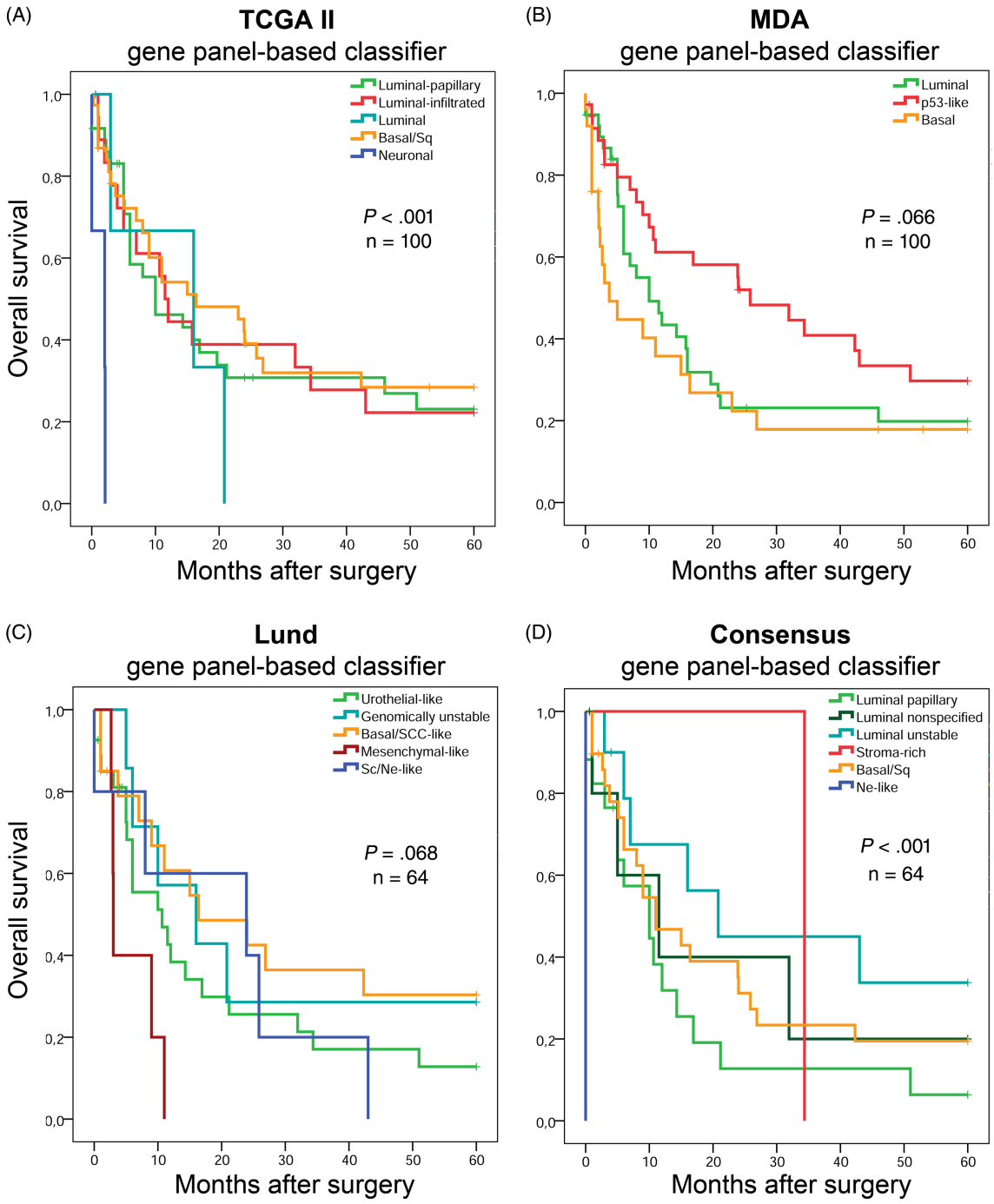

FIGURE 3 Cancer-specific survival stratified by molecular subtypes based on TCGA II (A), MDA (B), Lund (C) and Consensus (D) gene-panel based classifiers on our institutional cohort. Basal/Sq, basal/squamous; MDA, MD Anderson; Ne-like, neuroendocrine-like; Sc/Ne-like, small-cell/neuroendocrine-like; TCGA, The Cancer Genome Atlas [Color figure can be viewed at wileyonlinelibrary.com]

Our consensus classifier rule set revealed a significantly different survival in various consensus subtypes both in the in silico TCGA ($P = .047$) and our institutional cohort ($P < .001$) (Figure S5C,D).

Molecular subtypes determined by our gene panel-based classifiers were also correlated with CSS in our institutional cohort. TCGA II and Consensus classifiers proved to be prognostic ($P < .001$, $P < .001$) (Figure 3A,D), the neuronal subtype of the TCGA II, and the overlapping neuroendocrine-like subtype of the Consensus classification showed the worst CSS. Molecular subtypes stratified by MDA and Lund classifiers also resulted in borderline differences in CSS ($P = .066$ and $P = .068$) (Figure 3B,C).

4 | DISCUSSION

In the last few years, transcriptome analyses revealed a considerable molecular diversity of urothelial MIBC. These different gene expression patterns led to the definition of various molecular subtypes with

distinct clinical behavior and therapeutic sensitivity. As transcriptome-based methods—due to their complexity and high costs—are not compatible with daily clinical routine, a feasible and accurate method for molecular subtype classification is of great clinical importance. Therefore, efforts have been made to develop simplified methods, with typically 2 to 5 immunohistochemical (IHC) or 10 to 50 mRNA markers. Rinaldetti et al described a NanoString-based gene expression method with a 36-gene panel. MIBC samples from RC (n = 44) were classified into luminal, basal and p53-like subtypes. Interestingly, they found luminal subtype to be an independent risk factor for patients' survival.[18] Kardos et al transposed the BASE47 mRNA expression classifier[6] to a NanoString-based platform and divided samples into luminal and basal subtypes but could not observe a prognostic difference between these two groups.[19] Morera et al published an RT-qPCR-based method with a reduced gene panel in a RC-treated MIBC cohort (n = 39). They stratified luminal, luminal-like, basal and basal-like subtypes, without any prognostic relevance.[20] In conclusion, current mRNA-based studies with reduced marker sets classified patients into a limited number (2-4) of subtypes, which were rarely found to have prognostic relevance.

Sjödahl et al performed parallel mRNA- and protein expression-based molecular classifications according to the Lund system based on transcriptome analysis and IHC using 29 antibodies. They were able to reduce the protein marker set to a minimum of 13 markers and concluded that global mRNA clustering and tumor-cell phenotype analyses may lead to different groupings of MIBC samples.[12] Most of the IHC studies distinguished luminal, basal and double negative subgroups. Font et al revealed by their IHC study that basal/squamous tumors can be identified by four markers (as KRT5/6 and KRT14 high and FOXA1, GATA3 low) and that this tumor subtype is associated with better response to NAC.[21] A similar IHC study determined basal and luminal subtypes based on the expression of five proteins (KRT5/6, KRT14, KRT20, GATA3, UPK2), but found no prognostic difference between the groups.[22] A further IHC classifier was developed after a systematic marker selection based on the TCGA and MDA mRNA data sets. Finally, authors assessed protein expression of five genes and found that IHC analysis of only two proteins; GATA3 and KRT5/6 could identify the luminal and basal subtypes with an overlap of 80%[23] (Table S6).

Overall, IHC analyses have the advantage that they can be easily integrated into the clinical routine and allow direct correlation of protein expression with intratumoral localization and histomorphological characteristics such as tumor variants/subtypes, tumor/stroma-ratio, type and distribution of immune infiltration, amount of necrosis and other factors. In addition, IHC can take tumor heterogeneity into account by analysis of the spatial distribution of expressed proteins. On the other hand, IHC-based molecular subtype classification systems with only 2 to 5 proteins are limited to a rather preliminary classification into luminal and basal subtypes. The clinical value of this dichotomous classification may be limited according to large transcriptome-based studies that underlined the particular clinical importance of the distinction of smaller subgroups (eg, the neuronal or luminal-infiltrated) as these showed different sensitivities to certain therapies (eg, immune checkpoint inhibitor therapies).[11,24] Therefore, accurate identification of these smaller molecular subtypes is of great clinical significance.

Panel-based gene expression studies have some more advantages; (a) as these are performed at the mRNA level, their results are more comparable to those of transcriptome-based studies; (b) mRNA techniques allow the feasible analysis of a larger number of genes, thereby permitting a more detailed classification. On the other hand, mRNA-based analyses do not allow the evaluation of the intratumoral localization of expression; therefore, stromal contamination of tumor samples may significantly influence results. Furthermore, as mRNA-based methods yield relative expression values, they are only applicable for subtype classification when larger number of samples are measured and cannot be used for classification of few or single samples.

Our 68-gene based method is the first gene panel-based subtype classification method that has been developed and validated on respective transcriptome data sets making our results more comparable to those of transcriptome-based studies. Our in silico analyses revealed an overlap of 79% for the TCGA II subtype classification. However, the marker set was primarily designed to recapitulate the TCGA II system, but we also reached an overlap of 76%, 69% and 64% for the MDA, Lund and Consensus systems, respectively. One major advantage of our gene panel-based subtype classification method is that we were able to classify patients into different subtypes that were originally defined in previous transcriptome studies (5 subtypes TCGA II, 3 subtypes MDA, 5 subtypes Lund and 6 subtypes Consensus). Accordingly, our technique also enabled to classify patients into smaller subtypes, like the neuronal and luminal-infiltrated groups.

As a next step, using an RT-qPCR method, we determined mRNA expression of our 68-gene panel in frozen samples of 104 MIBC patients who were treated with RC in our institution. The method proved to be robust as only 4 of 104 samples had to be excluded because of quality issues, leaving 100 samples for classification by our classifier rule sets. Then, we compared the prognostic values of the four classification systems in our institutional cohort to those found in the original transcriptome-based studies. In our cohort, the neuronal and the luminal subtypes were associated with the worst survival, which was similar to the findings of the TCGA II study.[10] Neuronal subtype represents ~5% of all MIBCs but is associated with a devastating prognosis and poor response to NAC.[10,25] On the other hand, tumors assigned to this subtype may well respond to immune checkpoint inhibitor therapy.[24] Therefore, distinguishing the neuronal subgroup is of clinical importance, but former RT-qPCR or NanoString platform-based studies were not able to identify this subtype.

On the other hand, we could not confirm the favorable prognostic value of luminal-papillary subtype, described in the TCGA II study.[10] However, in a recent transcriptome-based study with 283 MIBC patients, the luminal-papillary subtype was also not associated with favorable survival.[26] When classifying our institutional cohort according to the MDA systems, we found the p53-like subgroup to have the most favorable prognosis, while the luminal subtype had a slightly better prognosis compared to the basal group, which is similar to that of was found in the MDA study.[7] When classifying our

institutional cohort according to the Lund system, the mesenchymal-like subtype proved to be associated with poor survival, which is similar to the findings of the Lund group on their cohort.[26] Finally, according to Consensus classification, the luminal unstable group had a better, while the neuroendocrine-like subtype had worst survival. Overall, various molecular subtype classifications performed on our institutional cohort provided generally similar prognostic stratifications to those found in the original, transcriptome-based studies, however, with some differences.

As signature scores are summarizing gene expressions assigned to certain tumor intrinsic and stromal cell type attributes, these may have prognostic implications. Therefore, we assessed the nine signature scores compromising 68 gene expressions and found high neuronal score to be associated with poor OS, while high stroma-related signature scores such as ECM, p53 and immune scores were associated with favorable prognosis. In contrast, tumor intrinsic signatures (luminal, basal, squamous) showed no prognostic significance. On the other hand, stromal cell content showed no correlation with patients' OS or CSS (data not shown), suggesting that quality (type) of stromal cells is more important than the quantity of this component. Multivariable analysis revealed lymph node positivity, high neuronal and low immune scores as independent risk factors for OS. In line with these results, Pfannstiel et al observed a favorable prognostic value for increased number of tumor-infiltrating lymphocytes in MIBC and an association between immune infiltration and molecular subtypes. They found tumors with basal subtype to exhibit the highest lymphocyte infiltration and immune-related gene expression, followed by luminal-infiltrated tumors. Accordingly, in our cohort the immune signature score was the highest in basal and luminal-infiltrated subtypes (Figure S7).[27] In accordance, Ikeda et al revealed that high tumor-associated immune cell status associated with significantly better CSS in MIBC patients.[22] In a further study, a newly defined stromal immunotype of MIBCs with high $CD8^+$ cytotoxic T cells and natural killer cells was significantly associated with better overall and recurrence-free survival as well.[28]

Limitations of our work are that our patient cohort may be less representative for some reason. (a) We used frozen tissue samples for our real-time PCR analysis, which were collected only when a rest material remained after taking samples for the routine histopathological evaluation possibly leading to overrepresentation of larger tumors. Accordingly, our cohort included higher rates of pT4 tumors and OS times were shorter compared to the other studies. (b) Only a relatively low rate of patients received postoperative chemotherapy which may influence survival analyses.

5 | CONCLUSIONS

In this study, we present a robust and feasible RT-qPCR-based molecular subtype analysis method, which is able to recapitulate the TCGA II and the MDA classifications with an estimated overlap of ~80% and the Lund and Consensus classifications with 69% and 64%. Applying this method, we were able to classify 96% (100/104) of our institutional MIBC cohort and found a significant prognostic value for the TCGA II and MDA subtype classification systems. Furthermore, our method was able to identify smaller but clinically relevant subgroups (such as neuronal and luminal-infiltrated) which was formerly only possible by transcriptome-based analysis. Moreover, high stroma-related signature scores (ECM, p53, immune) were associated with favorable OS. In contrast, tumor intrinsic signature scores (basal, squamous, luminal) were not prognostic, except of neuronal score which—similar to immune score—proved to be an independent prognostic factor in MIBC. These results underline the importance of the molecular features of stromal component and suggesting that a dichotomous classification into basal and luminal subtypes may be of limited clinical value.

The final aim is to translate the findings of large transcriptome studies to a marker system that can be easily applied in the clinical routine using common platforms and robust assays. Our method needs to be transferred to formalin-fixed paraffin-embedded samples and be prospectively validated in independent patient cohorts also with regard to its predictive value for chemotherapy and/or immune therapy effectiveness prediction, which is the planned next step.

ACKNOWLEDGMENTS

We thank Dr Miklós Sárvári and Dr Attila Patócs for providing us the equipment for real-time PCR analyses and Dr Tibor Füle for his help in primary evaluation of real-time qPCR data. We are grateful to Dr Woonyoung Choi for providing subtype calls to publicly available MDA data set. Open Access funding enabled and organized by Projekt DEAL.

CONFLICT OF INTEREST

The authors declare no conflicts of interest.

DATA AVAILABILITY STATEMENT

Data sources and handling of the publicly available data sets used in this study are described in the Materials and Methods section and in Table 1. Further details and other data that support the findings of this study are available from the corresponding author upon request.

ETHICS STATEMENT

The study was performed according to the Declaration of Helsinki and the institutional ethics committee approved the study protocol (08-3942-BO/15-6400-BO).

ORCID

Csilla Olah https://orcid.org/0000-0002-4775-2432
Gottfrid Sjödahl https://orcid.org/0000-0002-7869-0473
Henning Reis https://orcid.org/0000-0003-1373-5295
Tibor Szarvas https://orcid.org/0000-0002-6321-0799

REFERENCES

1. Bray F, Ferlay J, Soerjomataram I. Global cancer statistics 2018: GLOBOCAN estimates of incidence and mortality worldwide for 36 cancers in 185 countries. *CA Cancer J Clin*. 2018;68:394-424.

2. Witjes JA, Bruins HM, Cathomas R, et al. European Association of Urology guidelines on muscle-invasive and metastatic bladder cancer: summary of the 2020 guidelines. *Eur Urol*. 2021;79:82-104.
3. Loriot Y, Necchi A, Park SH, et al. Erdafitinib in locally advanced or metastatic urothelial carcinoma. *N Engl J Med*. 2019;381:338-348.
4. Rosenberg JE, O'Donnell PH, Balar AV, et al. Pivotal trial of enfortumab vedotin in urothelial carcinoma after platinum and anti-programmed death 1/programmed death ligand 1 therapy. *J Clin Oncol*. 2019;37:2592-2600.
5. Sjödahl G, Lauss M, Lövgren K, et al. A molecular taxonomy for urothelial carcinoma. *Clin Cancer Res*. 2012;18:3377-3368.
6. Damrauer JS, Hoadley KA, Chism DD, Fan C, Tiganelli CJ. Intrinsic subtypes of high-grade bladder cancer reflect the hallmarks of breast cancer biology. *Proc Natl Acad Sci U S A*. 2014;111:3110-3115.
7. Choi W, Porten S, Kim S, et al. Identification of distinct basal and luminal subtypes of muscle-invasive bladder cancer with different sensitivities to frontline chemotherapy. *Cancer Cell*. 2014;25:152-165.
8. Seiler R, Ashab HAD, Erho N, et al. Impact of molecular subtypes in muscle-invasive bladder cancer on predicting response and survival after neoadjuvant chemotherapy. *Eur Urol*. 2017;72:544-554.
9. Cancer Genome Atlas Research Network. Comprehensive molecular characterization of urothelial bladder carcinoma. *Nature*. 2014;507:315-322.
10. Robertson AG, Kim J, Al-Ahmadie H, Weinstein JN, Kwiatkowski DJ, Lerner SP. Comprehensive molecular characterization of muscle-invasive bladder cancer. *Cell*. 2017;171:540-556.
11. Kamoun A, de Reyniès A, Allory Y, et al. A consensus molecular classification of muscle-invasive bladder cancer. *Eur Urol*. 2020;77:420-433.
12. Sjödahl G, Eriksson P, Liedberg F, Höglund M. Molecular classification of urothelial carcinoma: global mRNA classification versus tumour-cell phenotype classification. *J Pathol*. 2017;242:113-125.
13. Dadhania V, Zhang M, Zhang L, et al. Meta-analysis of the luminal and basal subtypes of bladder cancer and the identification of signature immunohistochemical markers for clinical use. *EBioMedicine*. 2016;12:105-117.
14. Aine M, Eriksson P, Liedberg F, Sjödahl G, Höglund M. Biological determinants of bladder cancer gene expression subtypes. *Sci Rep*. 2015;5:10957.
15. Rebouissou S, Bernard-Pierrot I, De Reyniès A, et al. EGFR as a potential therapeutic target for a subset of muscle-invasive bladder cancers presenting a basal-like phenotype. *Sci Transl Med*. 2014;6:244ra91.
16. Riester M, Taylor JM, Feifer A, et al. Combination of a novel gene expression signature with a clinical nomogram improves the prediction of survival in high-risk bladder cancer. *Clin Cancer Res*. 2012;18:1323-1333.
17. Szarvas T, Becker M, vom Dorp F, et al. Matrix metalloproteinase-7 as a marker of metastasis and predictor of poor survival in bladder cancer. *Cancer Sci*. 2010;101:1300-1308.
18. Rinaldetti S, Rempel E, Worst TS, et al. Subclassification, survival prediction and drug target analyses of chemotherapy-naïve muscle-invasive bladder cancer with a molecular screening. *Oncotarget*. 2018;9:25935-25945.
19. Kardos J, Rose TL, Manocha U, et al. Development and validation of a NanoString BASE47 bladder cancer gene classifier. *PLoS One*. 2020;15:e0243935.
20. Morera DS, Hasanali SL, Belew D, et al. Clinical parameters outperform molecular subtypes for predicting outcome in bladder cancer: results from multiple cohorts, including TCGA. *J Urol*. 2020;203:62-72.
21. Font A, Domènech M, Benítez R, et al. Immunohistochemistry-based taxonomical classification of bladder cancer predicts response to neoadjuvant chemotherapy. *Cancer*. 2020;12:1784.
22. Ikeda J, Ohe C. Comprehensive pathological assessment of histological subtypes, molecular subtypes based on immunohistochemistry, and tumor-associated immune cell status in muscle-invasive bladder cancer. *Pathol Int*. 2020;71:173-182.
23. Guo CC, Bondaruk J, Yao H, et al. Assessment of luminal and basal phenotypes in bladder cancer. *Sci Rep*. 2020;10:9743.
24. Kim J, Kwiatkowski D, McConkey DJ, et al. The Cancer Genome Atlas expression subtypes stratify response to checkpoint inhibition in advanced urothelial cancer and identify a subset of patients with high survival probability. *Eur Urol*. 2019;75:961-964.
25. Grivas P, Bismar TA, Alva AS, et al. Validation of a neuroendocrine-like classifier confirms poor outcomes in patients with bladder cancer treated with cisplatin-based neoadjuvant chemotherapy. *Urol Oncol*. 2019;38:262-268.
26. Kollberg P, Chebil G, Eriksson P, Sjödahl G, Liedberg F. Molecular subtypes applied to a population-based modern cystectomy series do not predict cancer-specific survival. *Urol Oncol*. 2019;37:791-799.
27. Pfannstiel C, Strissel PL, Chiappinelli KB, et al. The tumor immune microenvironment drives a prognostic relevance that correlates with bladder cancer subtypes. *Cancer Immunol Res*. 2019;7:923-938.
28. Fu H, Zhu Y, Wang Y, et al. Identification and validation of stromal immunotype predict survival and benefit from adjuvant chemotherapy in patients with muscle-invasive bladder cancer. *Clin Cancer Res*. 2018;24:3069-3078.

SUPPORTING INFORMATION

Additional supporting information may be found in the online version of the article at the publisher's website.

How to cite this article: Olah C, Hahnen C, Nagy N, et al. A quantitative polymerase chain reaction based method for molecular subtype classification of urinary bladder cancer—Stromal gene expressions show higher prognostic values than intrinsic tumor genes. *Int. J. Cancer*. 2022;150(5):856-867. doi: 10.1002/ijc.33809